„NoPig Metal-Loss Detection System for Non-Piggable-Pipelines“

Agreement No. DTRS56-03-T0006 dd. July 2003

Contractor: FINO AG, Germany

Final Report

January 2005

CONTENTS:

Abstract **4**

1. Introduction **5**

2. Field tests of NoPig system **5**

2.1. Tests in Canada **5**

2.1.1. Test June 2003 of TransCanada pipelines 5

2.1.2. Test November 2003 of TransCanada pipelines 5

2.1.3. Test November 2003 of TransGas pipelines 6

2.2. Tests in USA **6**

2.2.1. Test July 2003 of Marathon pipelines 6

2.2.2. Test July 2003 of Southern California Gas pipes 7

2.3. Status of NoPig system after tests **7**

3. Data collection on diverse defects **8**

3.1. Preparation of pipes **8**

3.2. Experimental results **8**

4. Hardware adaptations and improvements **9**

4.1. Sensor array **9**

4.2. Mobile unit **9**

4.3. Calibration **9**

4.4. Achieved improvements **10**

5. Numerical calculations of magnetic fields and modeling **10**

5.1. Calculation of magnetic fields outside a pipe **10**

5.1.1. 2D calculations of magnetic fields around endless pipes 11

5.1.2. Evaluation of the 3D eddy current solver Faraday 11

5.2. Calculation of output quantities of the NoPig system **12**

5.2.1. Simplified 3D calculations of defects with finite lengths 12

5.3. Definition of material parameters for modeling **13**

5.4. Modeling of ERW pipes **13**

5.4.1. Modeling of longitudinal seams 13

5.4.2. Modeling of pipes with a defect and a longitudinal seam 14

6. Building up of test facility **15**

6.1. Requirements and descriptions **15**

6.2. Resulting interference levels **15**

7. Development of a new post-processing algorithm **15**

7.1. Basic concept of data filtering for ERW pipes 15
7.2. Description of the filtering algorithm 16
8. Development of new post-processing programs 16
8.1. Program for calculation of transition functions and filtering 16
8.2. Program for field data evaluation 16
9. Examination of SoCal joint #3 welded together with joint #2 17
10. Comparison of single defects with multiple ones 18
10.1. Single defects in a long seam pipe 18
10.2. Transversal and longitudinal defect groups in a long seam pipe 19
11. Evaluation of the SoCal joints data with the new program 20
11.1. Joint #3 at 12 o'clock, and joint #2 at 3 o'clock 20
11.2. Joint #3 at 9 o'clock, and joint #2 at 12 o'clock 21
12. Differential magnetic field analysis 23
12.1. Displacements versus differential magnetic field analysis 23
12.2. DMF results for SoCal joints #3 and #2 24
13. Conclusions 25

Authors:

Guennadi S. Krivoi (Ph. D.)
J. Peter Kallmeyer
Andreas Baranyak

Hildesheim, January 2005

Abstract

In the project the digital filtering of NoPig displacement data is investigated and upgraded.

NoPig method is a non-destructive testing method for pipelines. NoPig is an above ground method for detecting and sizing wall thickness anomalies like corrosion in nonpiggable pipelines. It uses an applied current of various frequencies at two points along the pipeline up to 1 km apart. The magnetic field is measured above ground at inspection points along the pipe. Calculations use the measurement data to determine the deviation of an equivalent current line from central position called displacement. Due to the skin effect and the magnetic stray flux, a variation of the displacement with frequency indicates a local wall thickness reduction of the pipeline.

ERW-pipes produce an offset in displacements caused by different magnetic and electric properties in the area of long seams. This offset changes from joint to joint because the clock position of long seams in neighbor joints is different. In order to detect defects this offset must be filtered out.

The filtering procedure and software developed in this project allow to significantly enhance the probability of detection in ERW-pipelines by use of NoPig method. Additionally some upgrades were undertaken in the system itself which essentially reduced uncertainty in definition of displacements. After applying all upgrades 90% of artificial defects in an ERW-pipe were recognized.

1. Introduction

This is a final report about the works performed in the project summarizing the results. More detailed information about particular topics can be found in 5 Quarter Reports.

Corresponding to the project plan the project deliverables are:

1) Field trials 2003 Final Report including trials at TransCanada Pipeline, Marathon Ashland Pipeline and Southern California Gas Company
2) Description report for the upgrated software for specific project areas.
   - Improved evaluation software for specific project areas;
   - Evalution software determining adaptive filtering model;
   - Improved software after applications.
3) Quarterly status reports and final project report summarizing all project details.

2. Field tests of NoPig system

2.1. Tests in Canada

2.1.1. Test June 2003 of TransCanada pipelines

Between June 20th and June 24th, 2003 inspections of 12" Pipeline were performed. The test were done on the 12" Flat Lake Lateral pipeline at Vegreville, Alberta, Canada. 6 sections were inspected on this pipe.

A BJ MFL in-line inspection tool was run and the results were compared to the NoPig results. Excavations at various locations have also been completed. A close interval survey was also run to compare to NoPig´s current intensity measurements.

In total 5 "Detections below Level 1" were found. In section #1, #2, #5 and #6 no digging was performed, because the pig run did not indicate any defects larger than the NoPig reference defect. In section #2 at 89 m of NoPig distance a indication below level 1 corresponds with the pig run. At section #3 digs at 15 m and at 134 m were made. At both digs the indications given in the NoPig report are evoked from manufacturing tolerances in the pipeline.

At section #4 the 50% metal loss indication from NoPig corresponds to the 17% metal loss found by the ultrasonic inspection after digging out. From the pig run it was found 9% wall loss at the same position.

2.1.2. Test November 2003 of TransCanada pipelines

With the NoPig system it was inspected 3 sites on the "20" Marten Lateral near Edson, Alberta. These sites are titled site #11, site #5 and site #4 as given by TCPL. The inspections are done between October 27th to October 31th, 2003.

Only 2 features below level 1 were found at 80 m and 178 m in site #5. There are no indications that minimum coverage is below 0.8 m at any of the three sites. Digs were not yet performed on this pipe. All the swamp weights and the screw anchors are detected and indicated.

2.1.3. Test November 2003 of TransGas pipelines

The test was performed between November 3rd and November 4th 2003. The sites are near to Saskatoon. Site # 1 and site #3 had 14" and site #2 had 6" outer pipe diameter. The following NoPig inspection results were obtained:

Site #1:	116.25 m	feature, below 50 %
	The current intensity has a jump near to this position.	
	110 m – 116 m	increase of inspection current
Site #2:	48.25 m	feature below level 1
	234 m	feature below level 1
	90.25 m	weak current leakage
Site #3:	10.25 m	feature, 50% metal loss
	23 m	decrease of inspection current

At all sites the coverage of the pipe is more than 0.8 m.

For site #1 a comparison to the ILI data was made. At this side the excavation was made at app. 75350 m. A NoPig data shift of +13 m along the chainage aligns girth welds in vicinity of corrosion at 75300 m to 75370 m and aligns the deepest corrosion from ILI and excavations with the one and only NoPig metal loss call. Comparing the NoPig results to the ILI data it was found that all the girth welds are identified by NoPig. The uncertainty was within ± 1 meter.

2.2. Tests in USA

2.2.1. Test July 2003 of Marathon pipelines

2 – 10" Barge Dock Lines near to Mississippi river close St. Louis, Missouri, were inspected between June 30th and July 2nd. The lines are 2½ to 5 feet apart and therefore they are a good test of pipe separation specification. Fairly deep sections of pipeline were unable to be evaluated. Summary of the found indications:

Section #1:	28 m	Detection with 50% metal loss
	33 m	Detection with 60% metal loss.
	70 m – 74 m	Detection below level 1.
Section #4:	26 m	Detection below level 1.

In section #4 one detection below level 1 is found. This corresponds to the MFL data. The other MFL indications are in a region where the coverage is to deep for NoPig.

2.2.2. Test July 2003 of Southern California Gas pipes

Southern California Gas Test, Pico Rivera, California

Test was performed in Pico Rivera at facilities of SoCal between the July 8 and July 14. A lot of defects was machined with a casing cutter. The pipe diameter are with 8", 16", 20" and 24". In total 28 Inspection runs are made.

In this report only the 8" pipe with artificial defects will be described. Results about other pipe are described in inspection Final Reports. The 8"pipe is a combination of 4 joints. There are 16 artificial defects and 3 girth welds in the pipe. Table 1.1 presents an overview about the inspections on this pipe joints.

Table 1.1. Inspection runs on the 8" SoCal Pipe

o'clock position 1		**o'clock position 2**	
depth 1	**depth 2**	**depth 1**	**depth 2**
run 1	run 2	run 8	run 7

The data of the inspections were post-processed with a software used normally for seamless pipes. Only 45 % of all defects could be detected with this post-processing. The following features characterize the inspection results:

1. The long seam produces an offset in displacements which is nearly constant along a joint. At girth welds the offset has a jump because of changing clock position of the next joint. Used post-processing generates at this position side lobes. As result defects near to a girth weld are masked by these lobes.

2. Use of such post-processing leads to indication reduction. But in the raw data these indications are present at defect positions.

3. The positions of girth welds are very near to their exact positions. The deviation is lower than 0.25 m.

In totally 29 detections only 45% of all defects in the pipe were detected.

2.3. Status of NoPig system after tests

After inspections of artificial defects the surprise was that small defects could be detected, but some very large defects were undiscovered even in the raw data indications were present. Obviously this means that NoPig can detect defects but some circumstances like the constant offset along a pipe joint can mask the defect response.

The NoPig system and especially the post-processing software were developed for seamless pipes. The tests in Pico Riviera and the other locations were the first touch of the NoPig system with long seam welded pipes.

3. Data collection on diverse defects

3.1. Preparation of pipes

Table 3.1 presents an overview about all the inspected pipes and joints with artificial defects during the project.

Table 3.1. Data collection from diverse pipe joints with defects

No.	Pipe combination or pipe name	Date of inspection	Number of long seams	Number of clock positions	Coverage	Number of inspections	Section length rounded
0.	Pipe 1 (Rohr 31)	November 2003	1	3	0.75 m and 1 m	6	6 m
1.	Joint #1	June 2004	1	3	0.75 m	6	12 m
2.	Joint #2	June 2004	1	3	0.75 m	6	12 m
3.	Joint #3	June 2004	1	3	0.75 m	6	12 m
4.	Joint #4	June 2004	1	3	0.75 m	6	12 m
5.	Joint #1 and joint #3	July 2004	2	3	0.75 m and 1 m	36	24 m
6.	Joint #2 and joint #4	July 2004	2	3	0.75 m and 1 m	36	24 m
7.	Joint #1	August 2004	1	3	0.75 m and 1 m	6	12 m
8.	Fuchs pipe #1	August 2004	1	3	0.75 m and 1 m	6	17 m
9.	combination of joint #17, joint #16 and joint #18	August 2004	1	2	0.3 m, 0.75 m and 1 m	13	17 m
10.	GTS pipe #1 with single defects	November 2004	1	4	0.75 m and 1 m	8	17 m
11.	GTS pipe #1 with multiple defects	November 2004	1	4	0.75 m	4	17 m
12.	SoCal joint #3 with joint #2	December 2004	2	4	0.75 m and 1 m	8	24 m

These are in total 141 inspections. This corresponds to a pipeline length of 2911 m. Detailed descriptions can be found in the Quarterly Status Reports.

3.2. Experimental results

Pipe 1 (Rohr 31) was investigated more than described in table 3.1. On this seamless pipe all defects are detectable. Displacements of every defect are well known. Changes in the NoPig System or properties of test facilities were also characterized with this pipe.

Investigations of single joints from #1 to #4 were undertaken to understand the influence of the long seam. Inspections of welded pipe joints were performed to investigate joint

interfaces. These data are a background for the post-processing upgrade. The inspections are described in items 5, 6 and 12 in Table 3.1. Four different clock positions of long seam are investigated on 2 pairs of joints welded together.

One aspect of the project was the comparison of single and multiple defects. Therefore 2 defects were prepared in the GTS pipe #1. From initially 2 separated equal defects 2 different defect groups are build: a transversal one and a longitudinal one by addition of a second equal defect. The transversal defect group results in a reduction in the displacement of app. 50%. The longitudinal defect group results in an app. 25% increase of the displacement.

The Fuchs pipe #1 in Table 3.1, item 8, has 2 artificial defects. It was investigate to understand what defect dimensions are critical for detection at another wall thickness.

The combination of joint #17, joint #16 and joint #18 is an arrangement of different pipes. The joints are welded together. Pipe #17 and #18 are seamless. All the defects in the seamless joints could be detected. Pipe #16 is long seam with a 10 mm wall. The reference defect in the long seam pipe evokes a very weak signal.

The investigation of the SoCal joint #3 welded to joint #2 was necessary to obtain data with the improved NoPig system. 4 of 6 defects evoked indications in raw data. At the end of the project with the new post-processing more than 4 defects were detectable.

4. Hardware adaptations and improvements

4.1. Sensor array

The distance between magnetometer and magnetometer electronics was extended to 24”. The length of the connection cable between the sensor array and the mobile unit is extended to 24 feet. 24 new and more robust holders for the sensors were installed. NoPig software was upgraded. Each sensor is described with its own geometric positions.

The inspection current source is reduced to the half of the old size. The output current is 20% higher than before. That allows to enlarge the distance between 2 contact point on a pipeline to at least 1000 m.

4.2. Mobile unit

A low-pass antialiasing filter has been added between the sensor electronics and the A/D converter in the computer of the mobile unit. The aliasing interference caused by the fluxgate magnetometer excitation is thus suppressed. An upgraded rack to support computer, power supply, sensor electronics and the connection cables is manufactured. With the new rack it was possible to solve the problems with the ground loops in the DC power supply. The program in the data collector module is modified to collect the magnetic field data for each sensor additionally to traditional NoPig data.

4.3. Calibration

For the calibration procedure a more precise calibration table was manufactured. This supports a better reproducibility in the sensor array position and a more precise position between the sensor array and the calibration line. The more precise sensor adjustment

and the new calibration table allows to enlarge the calibration period to a few month instead of every inspection day. This increases the inspection length per day.

4.4. Achieved improvements

The target of all the hardware adaptations and improvements was to suppress system uncertainty and influence external interferences. As evidence of achieved improvements a comparison of the four-group formation in vertical displacements can be used. Below 3 different plots for the same joint are shown (from left to right): at the beginning (Pico Rivera blind test), in the middle, and at the end of the project.

Pico Rivera - blind test data July 2003	Hildesheim - same pipe June 2004	Hildesheim - same pipe Since August 2004
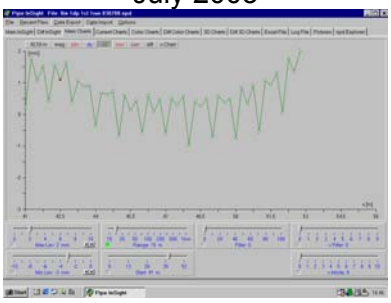		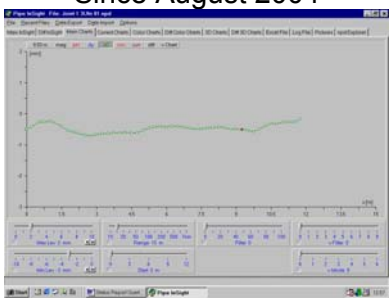

Figure. 4.1. Reduction of systematic errors in the vertical displacement of joint #1 during the project

The diagram shows a systematic reduction in the four-group formation. Finally, the current NoPig system has the following level of systematic errors expressed in displacements:

Four-group formation at the distance 0.75 m to the calibration line: $\lesssim$ 0,03 mm;
offset at the distance 0.75 m to the calibration line: $\lesssim$ 0,04 mm.

On a test facility some residual small interferences are present. These interferences were measured using as a test object just a copper cable. The copper cable was chosen because it has no own offsets or other kind parasitic displacements. Results for the test facility background displacements are as follows:

continuous offset along the cable	$\approx$ 0.13 mm
four-group formation	$\lesssim$ 0.03 mm
specific changing offset from the test area ground	$\lesssim$ 0.2 mm

5. Numerical calculations of magnetic fields and modeling

Numerical calculations were used to model the output of the NoPig system for different defects. The goal when using the numerical calculation is to reduce the number of experiments especially for the cases where an experimental investigation is rather complicated.

5.1. Calculation of magnetic fields outside a pipe

For a pipe with circular concentric cross-section the solving of the problem is trivial. But in the case of a pipe with a defect where the cross-section in the defect area is no more

circular and concentric, the solving becomes complicated. In this case, to solve the first problem the Maxwell's equations should be written for the pipe with a current including all the complicated geometry in the defect area. Two fundamentally different approaches can be used to solve these equations.

The first approach is to write the governing equation in differential form. The most used numerical technique to solve equations written in differential form is the finite element method (FEM). The second approach is to write the governing equation in integral form. Numerically the problem can then be solved by the boundary element method (BEM). Both of these methods have advantages and disadvantages depending on the geometry, material properties and the required accuracy of the final solution.

BEM has following advantages for the NoPig problem solving:

- High accuracy is attainable for magnetic fields. This is due to the field being calculated by integrating the solution.
- The problem does not have to be artificially truncated and a boundary condition applied to the artificial boundary.
- For linear problems unknowns are only located on the boundaries of the problem. This radically reduces mesh generation time and computer memory requirements.

There are two different kinds of software available from IES (Winnipeg, Manitoba, Canada) utilizing BEM. The first one called Oersted® is a 2D solver, and the second one, Faraday®, is a 3D solver.

5.1.1. 2D calculations of magnetic fields around endless pipes

For the calculation it is enough only to define a cross-section of the pipe, the current amplitude and the frequency. As a result of the solving the horizontal component of the magnetic flux density B_h for each sensor position is available. The obtained six magnetic field data are then stored in an output file. On this way a calculation for one of desired frequencies is obtained. This procedure must be repeated for each frequency of interest.

5.1.2. Evaluation of the 3D eddy current solver Faraday

In coordination with the developer and supplier IES of the 3D software Faraday for the AC magnetic field calculation the necessary trials were performed.

A trapezoid infinite defect was used as a modeling object. First, with Faraday, a simplified case with no material in the pipe was calculated. In Faraday it is possible to assign only current with no material. In this case that means that the assigned current is let flow by geometric considerations. As a “sanity check” the integral of *H*dl* was computed around a circle of the radius 500 mm. This works out to the current enclosed to about 10^{-6}A. This means that sanity check shows sufficient precision.

The second check was performed introducing material properties: magnetic permeability μ and electric conductivity σ. However, it was the attempt to accurately model current through a material with permeability and conductivity that was found not properly working in Faraday (version 6.1). With this version it was not going to be acceptable. Even reducing the length of the pipe to the portion where the current will not be flowing uniformly (the rest can be added as a simple assigned current) no satisfied results in the precision

were achieved. Even in the case of a pipe without any defect or long seam the *H* plot along the pipe has shown too large variations (about 10 %) that any effect of the defect will be lost in these calculation errors. Obviously, the program has problems with the spatial current distribution inside of a ferromagnetic material in the case where current flows.

Since September 2004 the evaluation of the upgraded version 6.2 Beta of the 3D hybrid eddy current solver Faraday was started. Sanity checks were running with simple objects like pipe without any defects to prove the precision of the software in the required frequency range. Unfortunately the desirable precision was still not reached. IES was informed about the problem and software developers are still working on the program in order to eliminate program bugs and reach the necessary precision.

5.2. Calculation of output quantities of the NoPig system

From the magnetic field solution obtained using Oersted the magnetic field density values B_j at the measuring points are calculated. Here *j* – the index of a sensor in the line of the NoPig sensor array. From these magnetic field data in the NoPig system the distance Z_f between the sensor line and the imaginary current line and its horizontal position Y_f are calculated. The index *f* denotes the frequency. This imaginary current line represents the simplest model of the pipe with the current as an infinitely thin wire leading the current. The differences between the distances Z_f, Y_f at different frequencies are called respectively vertical and horizontal displacements and are the "output" of the NoPig system. The vertical one is called ΔZ and horizontal one is called ΔY. The simulation program calculates both displacements using the same algorithm like the NoPig system does. As the final result of the modeling the curves $\Delta Z(f)$ and $\Delta Y(f)$ are obtained. This resulting plot models the output of the NoPig system in the case of an infinite defect.

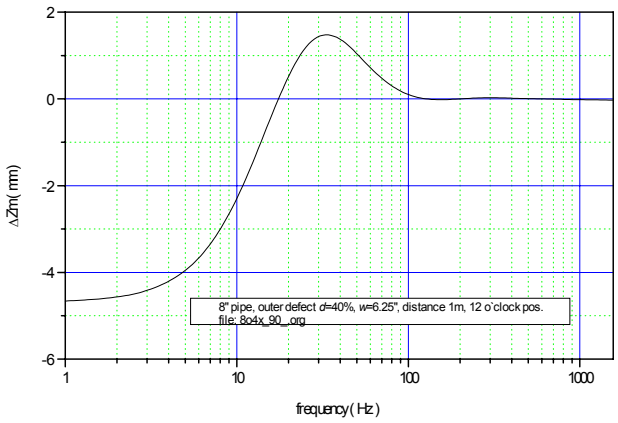

Figure 5.1. Modeled vertical displacement ΔZ_m for an infinite outer defect in 8" pipe with width w = 6½", depth d = 40%, and the distance Z_m = 1 m. Index "m" means "modeling".

5.2.1. Simplified 3D calculations of defects with finite lengths

In order to estimate the values of displacements for real situations where the defect length is limited, a fitting model was developed using Mathcad® software by Mathsoft. In Fig. 5.2

an example of modeling for the lowest frequency (8.5 Hz) is shown: the vertical displacement for a short defect with parameters 100 mm long, 50 mm wide and with 50% metal loss in an 8" pipe with the wall thickness 6.3 mm at 12 o'clock. The initial displacement for an endless defect with the same depth and width is 1.8 mm.

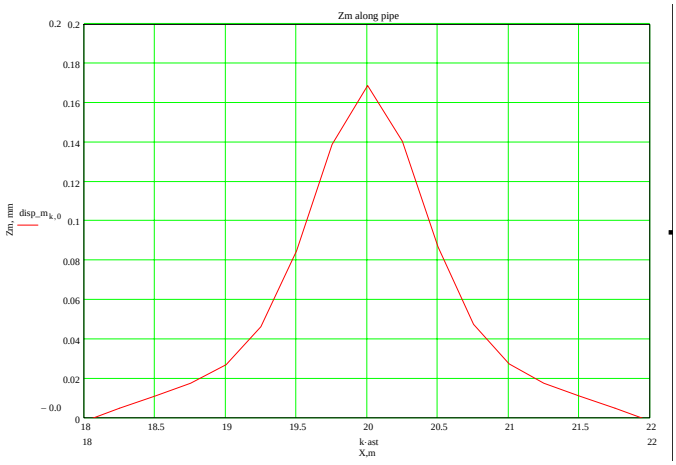

Figure 5.2. Modeling results of a short defect with parameters 100 mm x 50 mm x 50% metal loss at 12 o'clock.

5.3. Definition of material parameters for modeling

For the modeling with any eddy current solver like Oersted or Faraday knowledge about the electromagnetic parameters (relative magnetic permeability μ and electric conductivity σ) of pipeline steels is very important for obtaining reliable quantitative results. For definition of μ a setup was build for viewing and measuring of hysteresis curves of steel rings. The steel rings were cut off from pipes under test.

The frequency for measurements was chosen rather low (8.5 Hz) to avoid influence of the eddy current losses on measurements. Partial hysteretic curves were plotted and measured at different values of the magnetic field strength H and μ values were then calculated from the measured peak values of field B_m and strength H_m. The conductivity σ of steel rings was measured as well at 8.5 Hz using the 4-point technique for the resistance measurements. In the range of magnetic field strength used by NoPig method the found change of the permeability is relatively weak: from 140 to 190 for ERW pipes. The conductivity has even weaker variations.

5.4. Modeling of ERW pipes

5.4.1. Modeling of longitudinal seams

With the 2D-software Oersted, the magnetic fields were calculated for a pipe with a longitudinal seam. The longitudinal seam was simulated as a sector of the pipe wall with the width w which has different the magnetic permeability μ and the conductivity σ than the rest of the pipe wall. It was found that such a combination of parameters delivers the best fit: w = 20 mm, μ = 30 and $\sigma = 2 \times 10^6$ S/m.

For the modeling of longitudinal seams the 2D software is sufficient because the length of joints is normally 12 to 16 m, what is much more than the distance between the NoPig

sensor array and the pipe. Thus, the infinite case which is considered by Oersted can be successfully applied for such a length except in the joint ends and girth weld ranges. These transition regions need to be modeled using a real 3D software.

Based on the longitudinal seam modeling a visualization tool of long seams was developed. It allows to show the clock position of a long seam. The pipe is displayed in a "look through the pipe" (see Fig. 5.3). The tool allows scrolling through the pipe. The concentric grid allows for better defining the clock position of the long seam. The biggest circle of the grid corresponds to the position in the pipe closest to the viewer in the chosen range. The data shown in Fig. 5.3 were collected at two different clock positions of the long seam from an ERW-joint made by Fuchs. This new feature of the NoPig system can be used for the relation of ILI data to the chainage from above the ground because the NoPig x-coordinates are recorded much more precisely than the ILI points and have a certain relation to the coordinates on the surface like e.g., GPS.

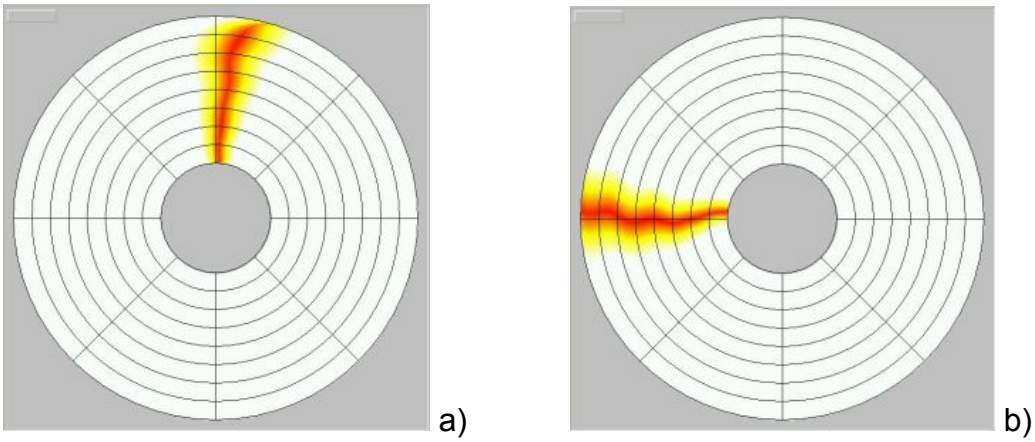
a) b)

Figure 5.3. Example of the long seam visualization: a) long seam at 12 o'clock, b) long seam at 9 o'clock.

5.4.2. Modeling of pipes with a defect and a longitudinal seam

The main idea for the new filtering algorithm is based on the analysis of properties of magnetic field deviations evoked by long seams. Long seams produced using ERW are characterized by homogeneous physical properties of the long seam area which are different from the rest of the pipe wall but rather constant along the seam. Under this presumption the middle range of a pipe joint should have rather constant displacements evoked by the long seam excepting areas where some defects can exist. Because the NoPig system has as a main goal to discover short defects, this means that displacements averaged over the whole middle range of a joint can only represent influences from the long seam even if a defect in this joint is present. Under this assumption, it is clear that subtraction of the averaged data over the middle range of a joint from initial data can retrieve displacements coming from defects.

This hypothesis was proven by applying of subtraction to modeled data. Displacement curves of longitudinal seams were subtracted from the displacement curves for the combination "defect + long seam" and resulting curves were then compared to the corresponding curves for isolated defects.

In this way, the displacement data evoked only by the defect were retrieved after subtraction. This shows that the subtraction of the background features formed by longitudinal seams can be used as thought before.

6. Building up of test facility

6.1. Requirements and descriptions

The area behind the NoPig office allows the inspection of pipe length shorter than 11 m. Another test facility was found. This test facility allows inspection of in total 27 m pipeline. The ground is stable enough to use a forklift changing the pipes. In the first time the sensor array was supported with wooden bars and plastic boxes. A platform supporting the sensor array was found more convenient. On this way the sensor array will be moved together with the platform by 2 workers. The pipeline was supported on wooden bars. Then turning of the pipe to other clock positions can be performed quickly and precisely.

Figure 6.1. Joint #2 with joint #3 on test facility with platform to simulate pipeline coverage.

6.2. Resulting interference levels

The results in the background displacements after all the hardware adaptations and improvements are:

continuous offset along the cable	$\approx$ 0.13 mm
four group formation	$\leq$ 0.03 mm
specific changing offset from the test area ground	$\leq$ 0.2 mm

7. Development of a new post-processing algorithm

7.1. Basic concept of data filtering for ERW pipes

The basic concept of the filtering algorithm was proven using the above reported modeling (see paragraph 5.4). This concept is based on subtraction of displacement curves evoked by long seams from initial displacement curves. This approach can be applied only in middle ranges of joints. A pipeline fraction around one joint is shown in Fig. 7.1.

Longitudinal ERW seams are marked as *LS* and girth welds are marked as *GW*. Due to pipeline construction requirements, long seams should be rotated from joint to joint as shown in Fig. 7.1. In NoPig displacements, it leads to a rather constant offset along the middle range *b* and a jump in offset in the transition ranges *a* and *c*. From experiments with SoCal pipes it is known that the length of transition ranges can be from 2 to 4 meter depending on the distance between the sensor array and the pipeline.

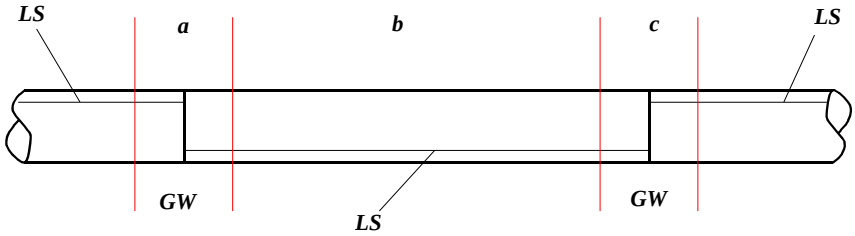

Figure 7.1. Fraction of a pipeline around one joint. *LS* – longitudinal seam, *GW* – girth weld, *a*, *c* transition ranges, *b* – middle range.

7.2. Description of the filtering algorithm

Based on this presumptions the following concept for the new filtering algorithm was formulated:

- finding out the girth welds positions based on the data offset jump analysis;
- separation of the middle range of every pipe joint;
- calculation of averaged offset features for these middle range;
- subtraction of these offset features from initial data; in this way data of middle ranges of joints will be filtered.
- calculation of transition curves for each transition range;
- subtraction of transition curves from initial data; in this way data of transition ranges will be filtered.

This algorithm was used for the development of the filtering program.

8. Development of new post-processing programs

8.1. Program for calculation of transition functions and filtering

For modeling the interface between two ERW joints a transition function must be calculated using a special developed filtering program. For the transition function calculation the following parameter are used: the depth of coverage and the length of the interface area. The program uses as input real NoPig displacement data file and calculates averaged values of the displacement offset along a joint. Then the program calculates transition curves for each NoPig measurement frequency and makes subtraction of them from the input data. Filtered on this way data will be thereafter stored in the standard NoPig format and can be analyzed with the standard NoPig evaluation software.

8.2. Program for field data evaluation

For the post processing and visualization of magnetic field data a new program called InField was developed. This program allows to perform calculations of magnetic field

deviations from available collected field data. Formulae for calculations must be defined by program user. This option provides the necessary flexibility for the filtering of data especially in the development period. The program allows calculation and displaying of results in both frequency and space domains. In the space domain the features can be compared along the pipe and along a sensor line. In the frequency domain these both space directions can be used as parameters.

9. Examination of SoCal joint #3 welded together with joint #2

Two reasons have made the inspection of joint #3 welded to joint #2 necessary.

1. The inspection data from the Pico Rivera test does not allow the new evaluation because of rather high systematic errors which are present in the Pico Rivera data.
2. Only with the upgraded NoPig system it is possible to pick up the magnetic field data simultaneously with collection of displacements data. Magnetic field data are necessary to use the Differential Magnetic Fields (DMF) analysis.

In Fig. 9.1 the displacements of joint #3 and joint #2 are presented. The first 2 m and the last 2 m are cut off because of the influenced from the cable connections. Fig. 9.1 shows displacements with a coverage of 1 m. In the first part of the vertical displacement a strong negative response at 8 m is present. A weaker response is at 5 m. At 10.9 m a very weak negative response is present in the vertical displacement. In the horizontal displacement a strong negative response is at 20 m. At 16.7 m a weak negative response is present. All these responses in the first part of pipe correspond to defect locations.

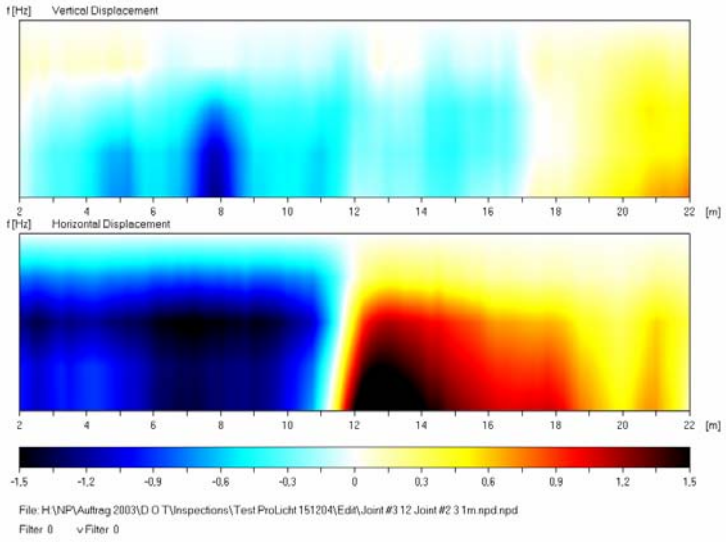

Figure 9.1. Data from joint #3 with defects at 12 o'clock welded together with joint #2 with its defects at 3 o'clock.

The change in the offset value at the girth weld position at 11.9 m has an influence on the defect responses at 10,9 m and 13.4 m. No responses from the defect at 13.4 m could be recognized. Most of the defects produce a response with an opposite sign than expected from theoretical considerations based on modeling of an infinite defect in a seamless pipe. We assume that it is caused by the long seam, but a detailed investigation is necessary to

clear this discrepancy. In Chapter 11 data from these joints are presented after the new filtering using transition functions for joints interfaces.

10. Comparison of single defects with multiple ones

10.1. Single defects in a long seam pipe

First 2 defects with a large distance in between are manufactured in the GTS Pipe #1. The dimensions are 100 mm diameter with 60% metal loss. The distance between is app. 4 m. They are considered as “single” or separated because the distance between the defects is larger than the distance between the pipe and the NoPig array. Fig. 10.1 gives a sketch about GTS Pipe 1 with single and multiple defects.

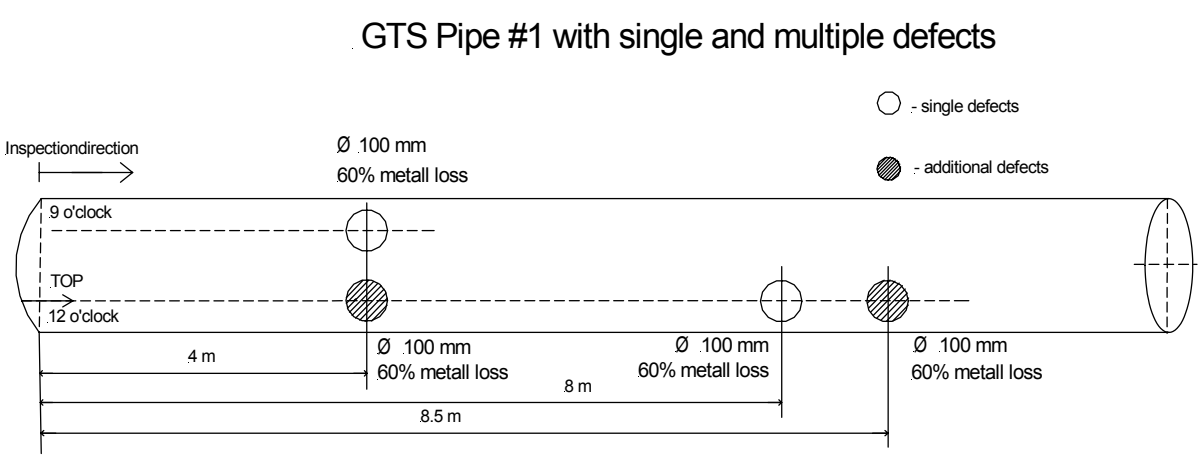

Figure 10.1. Sketch of GTS Pipe 1 with single and multiple defects.

In Fig. 10.2 the horizontal and vertical displacements of GTS Pipe #1 with single defects is presented as is. The coverage is app. 0.7 m. The data are not post processed or filtered.

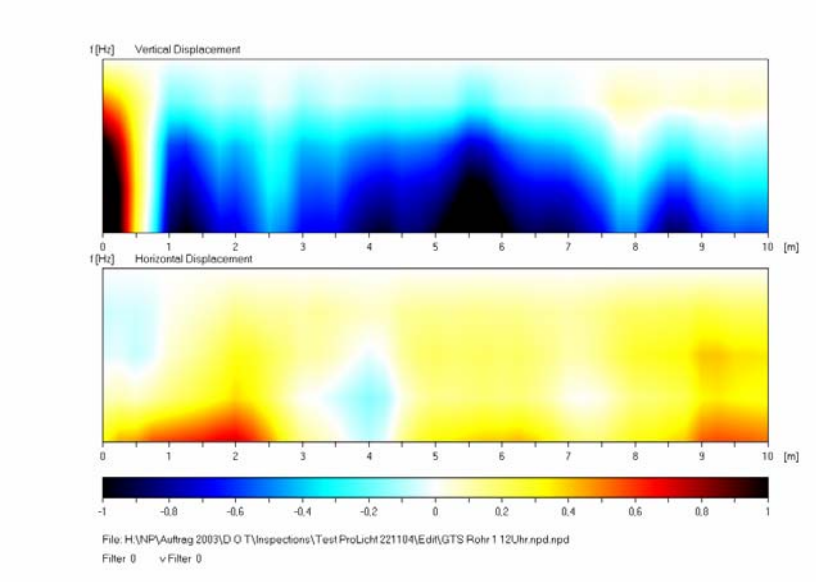

Figure 10.2. Data from GTS Pipe 1 with single defects at 0.7 m distance.

At 4 m a negative displacement (a light blue spot) is present in the horizontal displacement. The defect at this position is at 9 o'clock. At 8 m a displacement change toward the positive direction is seen in the vertical displacement. The defect at 8 m is at 12 o'clock. The displacement on the first 2 meters are influenced from the cable connections. The background offset in the vertical and horizontal displacements is caused by the long seam. The position of the long seam in GTS Pipe #1 is at 3 o'clock.

10.2. Transversal and longitudinal defect groups in a long seam pipe

After the investigation of the single defects the additional defects as shown in Fig. 10.1 are added in GTS Pipe 1. At the 4 m location another defect is added to the defect 1 in the transversal direction. Thus the first, transversal defect group is created. At the 8 m location an other defect is added to the defect 2 in the longitudinal direction.

The following Fig. 10.3. shows the vertical and horizontal displacements for the same pipe but with the described multiple defects. The horizontal displacement swing evoked by the transversal defect group at 4 m is smaller than the one from the single defect. In the vertical displacement a weak displacement change toward the positive direction is present in all the inspections.

The change in vertical displacement evoked by the longitudinal defect group from 8 to 8.5 meters is increased. The maximum of this change is shifted to 8.25 m. Thus the longitudinal defects act in displacements as a cluster contrary to the transversal defects. The latter weaken displacement changes because the circumferential asymmetry in the magnetic field characteristic of isolated defects is reduced if additional defects arise in the transversal direction.

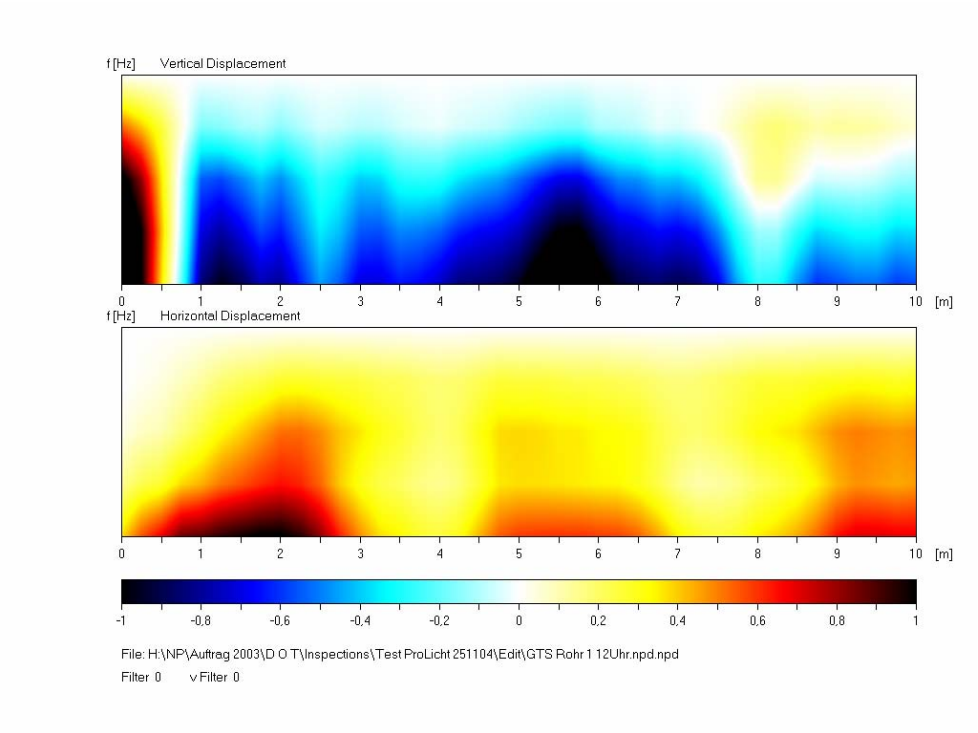

Figure 10.2. Data from GTS pipe #1 with multiple defects at 0.7 m distance.

Comparing the displacement in Fig. 10.1 with Fig. 10.2 it is seen that the displacement at the transversal defect group is reduced by app. 50%. The displacement at the longitudinal defect group is increased by 25%.

11. Evaluation of the SoCal joints data with the new program

The SoCal 8" ERW-joints #3 and #2 were welded together and then investigated with the NoPig system at NP Inspection Services test facilities. Rather strong offsets in both horizontal and vertical displacements mask defects. Use of the filtering program described in Chapter 8 allows us to reduce these offsets. All the data presented here were collected at about 1 m distance between the NoPig sensor array and the axis of the pipe.

Further it is shown how the new filtering program can be applied for evaluation of data for this joint combination when they are at two rotation positions: (i) joint #3 at 12 o'clock, and joint #2 at 3 o'clock; and (ii) joint #3 at 9 o'clock, and joint #2 at 12 o'clock. The description of defects is given in Table 11.1. In the surface plots presented below the X-range is shown only from 2 to 22 meters because the data from the beginning and the end of pipe are influenced by cable connections.

11.1. Joint #3 at 12 o'clock, and joint #2 at 3 o'clock

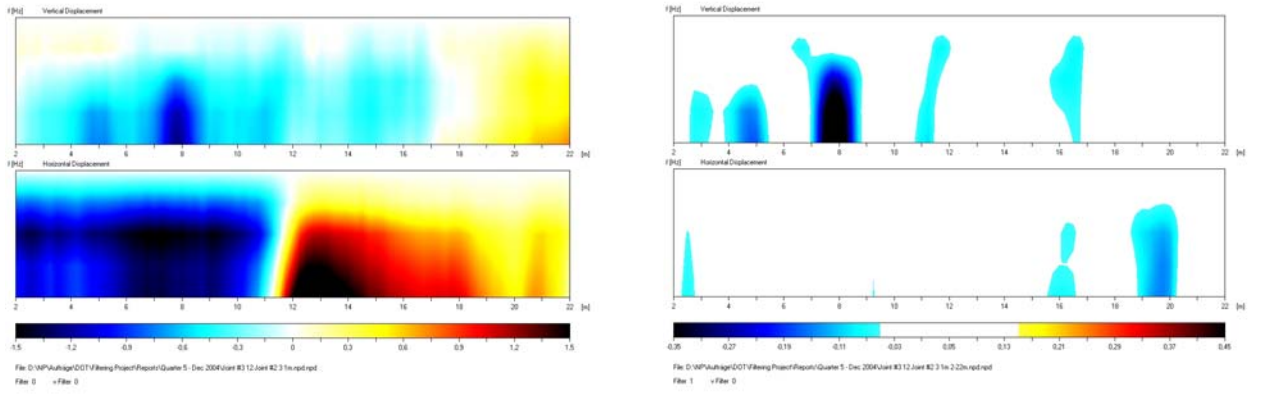

a) b)

Figure 11.1. Displacement data: a) before filtering, b) after filtering.

Joint #3 is from 0 to 11.88 m, and joint #2 – from 11.88 m to the end of pipe. In the case shown in Fig. 11.1 the defects in joint #3 are at 12 o'clock, and the ones in joint #2 – at 3 o'clock. Thus responses from defects are expected to be in the vertical displacement for joint #3, and in the horizontal displacement for joint #2. In Fig. 11.1a following defects can be recognized: (i) joint #3: defect 3.3 at 5.03 m, defect 3.4 at 7.89 m, and defect 3.5 – very weak; (ii) joint #2: only defect 2.3. Responses from defects 2.1 and 2.2 are masked with interface (2.1) and offset (2.2). Note that responses have opposite sign than expected from the theoretical consideration. As a possible explanation for this the influence of long seam can considered, but it needs more detailed investigations.

The results after filtering are shown in Fig. 11.1b. For a better defect recognition on the background of residual noise a smoothing filter over 3 points (including the actual point) was applied as well as a threshold level. Reduced levels are marked on the scale on the

bottom of plots as the white range. The defects 3.3, 3.4, 3.5, and 2.3 can be clearly recognized, and additionally the defect 2.2 can be found. It produces responses in both vertical and horizontal displacements even its reaction is expected to be only in the horizontal direction. Probably there is a slight shift of the defect from the exact 12 o'clock position. The defect 2.1 can not still be detected (it is located at 13.42 m at 3 o'clock). We assume that is because of its small dimensions.

11.2. Joint #3 at 9 o'clock, and joint #2 at 12 o'clock

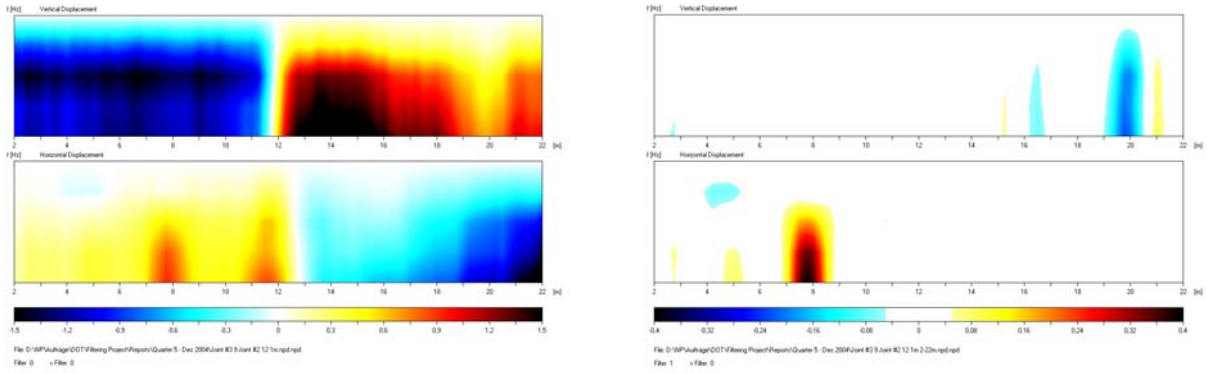

a) b)

Figure 11.2. Displacement data: a) before filtering, b) after filtering.

In this clock position responses from defects are expected to be in the horizontal displacement for joint #3, and in the vertical displacement for joint #2. In Fig. 11.2a following defects can be recognized: (i) joint #3: defect 3.4 at 7.89 m, and defect 3.5 is masked with the response from the girth weld; (ii) joint #2: only defect 2.3. Also here responses from defects 2.1 and 2.2 are masked with the joints interface (2.1) and offset (2.2). After filtering (see Fig. 11.2b) defects 3.3 and 2.2 additionally were recovered.

Results from both rotation positions of these welded joints are summarized in Table 11.1. It was analyzed 6 different defects, each defect at 2 different clock positions. From these 6 defects 4 were detected at each clock position, and one defect (defect 3.5) was detected only at 12 o'clock. One defect (defect 2.1) was not detected at all. But this defect is too short, lying in the length below NoPig specifications. Thus for estimation of percentage of detected defects only 5 defects must be taken. In this case the common number of trials is 10 (5 defects, each in two clock positions), and the common number of recognized defects in these 10 trials is 9, that means 90%.

For comparison: in the evaluation 2003 of the Pico Rivera data with the corresponding depth of coverage only defect 3.4 was certainly detected one time. Other detections either had false X-coordinate deviating more then by 1 m from the real defect locations (3 detections) or were even not recognized.

False responses from the girth weld are effectively reduced due to the new filtering. The old filtering used in 2003 for the evaluation of Pico Rivera data had such false responses covering a rather wide range of about 4 to 5 m around the girth weld.

Table 11.1. Results of defect detection after filtering for 8-inch SoCal joints #3 and #2.

Joint No.	Defect No.	Defect parameters				O'clock positions	
		Length [mm (in)]	**Width** [mm (in)]	**Depth** (%)	**Location** (m)	**Joint #3:** 12 o'cl. **Joint #2:** 3 o'cl.	**Joint #3:** 9 o'cl **Joint #2:** 12 o'cl
3	3.3	108 (4 ¼)	121 (4 ¾)	54	5.03	detected	detected
	3.4	102 (4)	184 (7 ¼)	60	7.89	detected	detected
	3.5	64 (2 ½)	95 (3 ¼)	55	10.90	detected	-
Girth weld	GW	-	-	-	11.88	detected	detected
2	2.1	45 (1 ¾)	29 (1 1/8)	66	13.42	-	-
	2.2	146 (5 ¾)	25 (1)	54	16.79	detected	detected
	2.3	32 (1 ¼)	83 (3 ¼)	66	19.96	detected	detected

12. Differential magnetic field analysis

12.1. Displacements versus differential magnetic field analysis

In the NoPig system during pipeline inspection the magnetic field induced by the inspection current flowing through the pipeline will be measured by the sensor array consisting of four sensor lines each containing 6 sensors. The inspection current contains multiple frequency components. Spectral densities of the magnetic field taken for one of the frequency component and for one sensor line are used in the NoPig system for the calculation of the distance between the sensor line and the position of an virtual current lead substituting the pipeline. This simple model used in the NoPig system for the magnetic field simulation requires concentric and circular fields for every frequency used in the NoPig method. If a current lead is used as a substitute for a pipeline with the same current, the frequency-dependent displacement appears in the case of an anomaly in the wall of the pipe. This displacement is considered in NoPig method in Cartesian coordinates as consisting of two components: vertical and horizontal ones.

The problem is that real magnetic fields from pipelines are neither circular nor concentric even in cases without any defect when they are just made of long seam joints. Modeling with Oersted described above has shown that even for a simple model of the long seam as a sector with different values μ and σ the shape of the magnetic field is more egg-like than circular one. In Fig. 12.1 plots are shown for deviations of the magnetic field amplitude from the case of circular field.

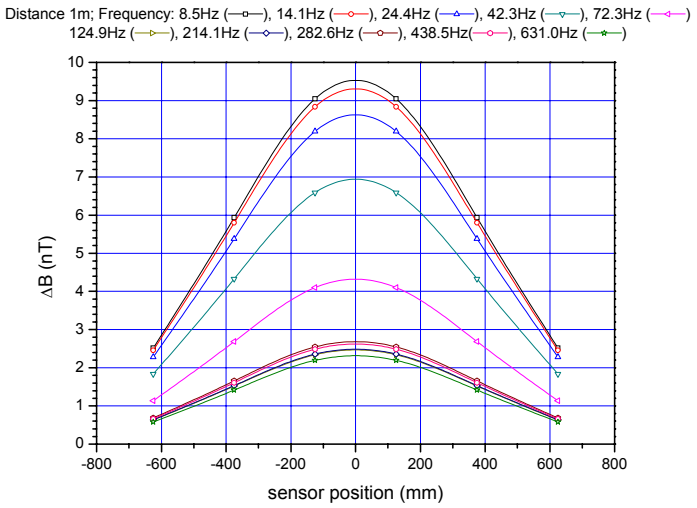

Figure 12.1. Calculated deviations of the magnetic field amplitude ΔB for a long seam 8“ pipe from the case of the circular and concentric magnetic field.

These curves are calculated for a 8” pipe with a long seam at 12 o’clock position at the distance 1 m between the pipe axis and the NoPig sensor array. The horizontal axis is the position along the sensor line of the array, and the vertical one is the deviation of the magnetic field amplitude from the case if the magnetic field lines were circular and concentric. The curves are calculated for 10 different frequencies in the range from 8.5 Hz to 631 Hz. Note that in the case of the circular and concentric field lines corresponds to the straight line at $\Delta B = 0$.

Let us consider, e.g., the curve for 8.5 Hz. In the NoPig system this curve can only be interpreted by a straight line at $\Delta B \cong 6$ nT for which a vertical displacement will be calculated. In this way the whole change of the magnetic field deviations in the range from 0 to 9.5 nT is obviously reduced. This leads to loss of the sensitivity of the method. Thus a direct analysis of the magnetic field data can improve the sensitivity of the NoPig method. In more complicated situations where not only a long seam is present but also a defect in an arbitrary clock position, the magnetic field deformation above the defect can be more complicated as just egg-like. In some situations this can lead to full loss of the sensitivity to the defect if analyzing displacements despite of the presence of magnetic field deviations in collected data.

Thus the deviations of magnetic field values similar to ones presented in Fig. 12.1 should be useful for data evaluation instead of calculation of displacements. By reason of impossibility to obtain magnetic field data of non-distorted magnetic field for every position of the sensor array along the pipe during inspection another reference for calculation of field deviations must be found. We consider magnetic field data for one of the frequencies, say the highest one, as a good alternative for this purpose.

For realization of this new method which will be called Differential Magnetic Field (DMF) analysis the magnetic field data should be collected during inspection for every working frequency and every sensor. Thereafter rather simple calculations to obtain field deviations should be performed. Calculations of distances between the array and the pipeline and the current in it must be performed as before because these data are important for customers. Collecting and storage of magnetic field data must be running parallel to traditional calculations. In the current NoPig system, this option is recently realized.

12.2. DMF results for SoCal joints #3 and #2

Presented DMF analysis is based on the differential comparison of magnetic field data obtained from every sensor of the NoPig system. Sensors are aligned in lines in the same direction. During inspection the middle of sensor array is positioned over the pipeline to be inspected so that the sensor lines are perpendicular to the pipe axis. Thus along a sensor line a symmetry in magnetic field values must exist if the pipe has no defect. The magnetic field produced by the inspection current flowing through the wall of the pipeline will be measured at different frequencies. Deviations of magnetic field values in both frequency and space domains must be analyzed to recognize defects. As indicators there are two parameters chosen: *u1* for defects lying mainly in the vertical plane and *u2* for defects lying mainly in the horizontal plane.

The definition of parameters is as follows:

$$u1 \equiv a4/a6\text{-}c4/c6 + a5/a6\text{-}c5/c6 - a4/a5\text{+}c4/c5 + a3/a1\text{-}c3/c1 + a2/a1\text{-}c2/c1 - a3/a2\text{+}c3/c2, \quad (1)$$

$$u2 \equiv a1/a6\text{-}c1/c6\text{-}a2/a5\text{+}c2/c5\text{+}a3/a4 - c3/c4, \quad (2)$$

where *a1…a6* and are differences of sensors output signals in terms of the magnetic field at each frequency, and *c1…c6* are similar differences but only at the reference frequency.

The parameters *u1* and *u2* are chosen to be substitutes of the vertical and horizontal displacements, correspondingly.

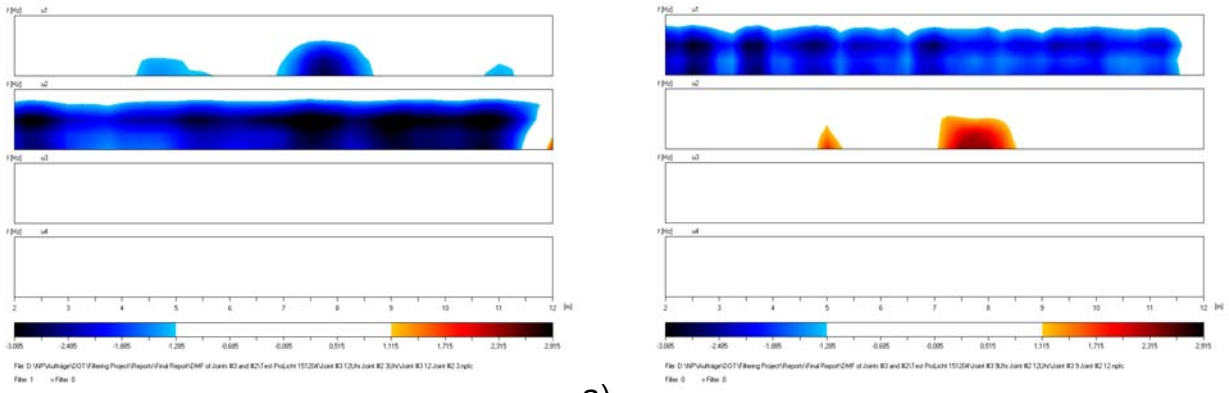

a) b)

Figure 12.1. DMF analysis results: a) for 12 o'clock defect position, b) for 9 o'clock defect position.

The results for SoCal joint #3 at two different clock positions are shown in Fig. 12.1. This ERW-pipe has 3 defects which could be detected: 3.3, 3.4, and 3.5 (see defects description in Table 11.1). In Fig.12.1 the responses are clear from all three defects in the parameter *u1* plot because the defects are at 12 o'clock thus in the vertical plane. In the horizontal plane the offset from longitudinal weld is present like in horizontal displacements.

When the pipe is rotated so that defects are at 9 o'clock position the responses from defects occur in the parameter *u2* plot. Just defects 3.3 and 3.4 can be recognized. The reduction of the response from the defect 3.5 can be caused by influence of the neighbor girth weld (at 11.88 m). In the *u1* parameter plot the offset is present again. The data were not filtered to reduce offsets either in the middle regions of joints or in transition regions around the girth weld. We used here the joint #3 which has a minimal offset in the plane where the defects are. Residual offset could be easily reduced by using of noise reduction filters (white zone in the color scale). The filtering approach for ERW-pipes developed for displacements in this project can be applied for parameters *u1* and *u2* as well but a corresponding software is not yet developed.

From plots it is seen that the defects can be clearly recognized using DMF. DMF analysis delivers more contrast between defect/no defect zones of a pipeline.

13. Conclusions

All the tasks of the project were fulfilled. The hardware and software of the NoPig system were upgraded what resulted in a significant reduction of systematic errors and uncertainty of definition of displacements. A new filtering algorithm intended for offset reduction in displacement data obtained from inspections of ERW-pipes was developed, investigated and used for development of a new filtering program. This new filtering program was applied for evaluation of NoPig displacement data for the same ERW-joints as in the test in Pico Rivera in 2003. In 2003 from 10 considered possible indications only one detection was achieved.

The filtering procedure and software developed in this project allow to significantly enhance the probability of detection in ERW-pipelines by use of NoPig method. Additionally some upgrades were undertaken in the system itself which essentially

reduced uncertainty in definition of displacements. After applying all upgrades 90% of artificial defects in an ERW-pipe were recognized.

Additionally in the project a new data collection and evaluation method was sampled: the DMF analysis – Differential Magnetic Field analysis which promises a better resolution of small defects on the background of magnetic field distortions which are normal for ERW-pipes.

Many thanks to all the project participants especially to Southern California Gas Co., and N.V. Nederlandse Gasunie, The Netherlands for sending their pipes.